



Methodological approach for mapping the flood physical vulnerability index with geographical open-source data: an example in a small-middle city (Ponferrada, Spain)

Laura Tascón-González¹ · Montserrat Ferrer-Julà¹  · Eduardo García-Meléndez¹

Received: 27 January 2023 / Accepted: 5 December 2023
© The Author(s) 2024

Abstract

To increase the resilience of communities against floods, it is necessary to develop methodologies to estimate the vulnerability. The concept of vulnerability is multidimensional, but most flood vulnerability studies have focused only on the social approach. Nevertheless, in recent years, following seismic analysis, the physical point of view has increased its relevance. Therefore, the present study proposes a methodology to map the flood physical vulnerability and applies it using an index at urban parcel scale for a medium-sized town (Ponferrada, Spain). This index is based on multiple indicators fed by geographical open-source data, once they have been normalized and combined with different weights extracted from an Analytic Hierarchic Process. The results show a raster map of the physical vulnerability index that facilitates future emergency and flood risk management to diminish potential damages. A total of 22.7% of the urban parcels in the studied town present an index value higher than 0.4, which is considered highly vulnerable. The location of these urban parcels would have passed unnoticed without the use of open governmental datasets, when an average value would have been calculated for the overall municipality. Moreover, the building percentage covered by water was the most influential indicator in the study area, where the simulated flood was generated by an alleged dam break. The study exceeds the spatial constraints of collecting this type of data by direct interviews with inhabitants and allows for working with larger areas, identifying the physical buildings and infrastructure differences among the urban parcels.

Keywords Physical vulnerability indicators · Flood hazard · GIS · Open data · Cartography

✉ Montserrat Ferrer-Julà
mferj@unileon.es

Laura Tascón-González
lauratg88@hotmail.com

Eduardo García-Meléndez
egarm@unileon.es

¹ Research Group on Environmental Geology, Quaternary and Geodiversity (Q-GEO), Biological and Environmental Sciences Faculty, Universidad de León, Campus de Vegazana, sn, 24072 León, Spain

1 Introduction

The interaction of natural phenomena with humans does not affect all societies in the same way. The amount of social, economic, material and environmental losses is proportional to the vulnerability of lands and communities (Vargas 2002). Since the middle of the twentieth century, when the concept of vulnerability was introduced in the risk analysis terminology, the definition of vulnerability has evolved. These changes have been based on (i) the characteristics of the community where it has been applied and (ii) the moment when it has been defined. Therefore, the new meanings of vulnerability correspond to the different ways of conceptualizing and quantifying it. In this way, each new definition has added new content (Weichselgartner 2001; Fuchs et al. 2007).

This means that when a new study related to this subject begins, the initial step is to define the term vulnerability. In the present study, the definition is based on the precedent characterization performed by UNDRO (1980), Vargas (2002) and Kumpulainen (2006). In this way, vulnerability has been considered as the susceptibility of an element or group of elements under risk that is the result of a natural or anthropogenic hazard of a determined magnitude. It is important to note that this vulnerability is measured on a scale ranging between 0 and 1 and is estimated by two components. The first is the degree of exposure faced by social, physical, economic and environmental factors. The second is the capacity for resistance against the phenomena. This resistance includes the capacity of protection and immediate reaction and the capacity of recuperation or resilience (Tascón-González 2017). This last term is defined as “the capacity of a system, community or society exposed to a threat to resist, absorb, adapt and recover from its effects in a timely and effective manner, which includes the preservation and restoration of its basic structures and functions” (UNISDR 2005). Therefore, this definition considers resilience as a factor of the vulnerability (Berkes 2007), in contrast to those authors who consider the resilience as an antonym to vulnerability (Adger 2000). Then, it is important to know how to identify, manage and reduce disasters, but most of them are unavoidable and the only way out to diminish the effects of these phenomena is to increase the resilience of the society.

The vulnerability of societies has increased in recent decades (Lundgren and Jonsson 2012). The main reason is the population growth and the extension of the infrastructure network over traditional flood areas that previously have not been human-occupied. Consequently, this incursion has meant an increase in exposure of the societies. The communities and their belongings have become weaker than before and may be hit more often by extreme events. At the same time, the population is changing their risk perception, and they feel that the number of extreme events is rising. This new awareness stems from the development of new technologies and the free circulation of information. Both allow the detection and knowledge of any natural event that occurs at any point of the globe and give the impression that the frequency of extreme events is increasing (Velev and Zlateva 2012; Kryvasheyev et al. 2016; Sim et al. 2018; Wang and Ye 2018). This means that not always there is an increment in the number of extreme events but in the number of people and beings exposed to them and in the spreading of information.

Vulnerability is a multidimensional concept. For this reason, estimating the vulnerability of a hazard may be analysed from different points of view, mainly economic, social, environmental, physical, administrative or political. In some societies, the main view could even be religious (Gaillard and Texier 2010; Gianisa and Le De 2018). To address all these interpretations, the best method is to evaluate each vulnerability type by a group of factors. The primary characteristic of these factors is that they are

observable and identifiable before an event occurs. This situation leads the society to study the factor through the prevention, prediction and reduction of the vulnerability to counteract its negative influence. Possible factors in social vulnerability include age, foreign population and disabled residents (Kappes et al. 2012; Dunning and Durden 2013; Terti et al. 2015; Aksha et al. 2019).

At the same time, factors are informed by different indicators (Balica et al. 2009). An indicator is defined as a variable that captures the factor's condition or part of it in a determined place and time. In general, indicators are statistical data that synthesize the primary information that the factors describe. Due to the difficulty of achieving this goal with just one indicator, in most cases, two or more indicators are used to define one factor. Therefore, the best indicator is the variable that summarizes or simplifies basic information, makes visible a phenomenon of interest and quantifies, and measures and communicates relevant information (Gallopín 1997). Following the abovementioned social factors, as an example, a possible indicator of foreign population would be the percentage of foreigners or the number of tourists per each 10,000 inhabitants.

So far, the literature shows that social vulnerability is the most common approach treated in risk analysis (Scheur et al. 2011; Koks et al. 2014; De Loyola et al. 2016; Noradika and Lee 2017; Tascón-González et al. 2020). Nevertheless, interest in physical vulnerability is growing. It has a long tradition in seismic risk analysis, and this approach is spreading over other hazards such as floods (Creach et al. 2016; Mazzorana et al. 2014; Bigi et al. 2021). Physical vulnerability focuses on the response of buildings and infrastructures or basic elements when a hazard occurs (Papathoma-Köhle et al. 2022). Consequently, the main analysed factors are building age, building material, building height, and the existence of infrastructure networks related to telecommunication, energy and transportation (Bisbal et al. 2006; Holand et al. 2011; FEMA 2011; Miranda and Ferreira 2019; Malgwi et al. 2020; Usman et al. 2021; Malakar and Rai 2022). These last ones are the set of services over which the productive structure of a society is based. They facilitate services, consumption activities and social relationships, which allow regional development and quality of life.

The implementation of this type of analysis demands large amounts of data. Some of them belong to citizens, so field enquiries are needed. This can be done when the number of buildings is low, but it can only be afforded by companies (such insurance companies) or Governmental Administration when the study area is a town. Other type of data is stored in governmental datasets. Since 2009, there has been an important movement among Governmental Administrations to give open access to their data (Abdelrahman 2021). This has led to the creation of the International Open Data Charter (ODC 2015) in which 170 countries agreed to several principles as a frame of norms for how to publish governmental and public data. These principles could be summarised as follows:

- (1) Open by default: it remarks that Governments should justify when data are not opened in juxtaposition to the default closed data that they have offered until now.
- (2) Timely and comprehensive: open data only is valuable when they are published on time and in a comprehensive way.
- (3) Accessible and usable: data should be free of charge and easy to find as well as it should follow a well-known file format.
- (4) Comparable and interoperable: data should be stored following some standards and with metadata that allow comparing among different sources.

All of them should encourage transparency to improve government performance. At the same time, it is expected that the use of open data in enterprises promotes their innovation and economic development. This new scenario poses challenges to researchers to analyse the fitness of the large open government data in their studies, such as the physical vulnerability of a natural hazard.

Therefore, in this paper, we propose a method to map the physical vulnerability against floods and its implementation in a middle-sized town, Ponferrada (Spain). This city is located 10 km downstream of a dam. This proximity to the infrastructure means that the citizens of Ponferrada could suffer significant damage as a result of a potential dam break.

In contrast to other studies related to physical vulnerability, our analysis will not focus on the damage suffered by the infrastructures when the flood has already occurred, but it will estimate the real vulnerability and identify the weakest infrastructures against a flood before the event happens (Ezell 2007). The objective is to facilitate land planning and to prepare a resilient society.

Until now, most of the vulnerability results have been presented at the municipal scale (Weichselgartner 2002; Ruiz 2011; Aroca et al. 2017) or analysing buildings or infrastructures, but not both at the same time (Erena and Worku 2019; Singh et al. 2019; Cheng et al. 2022). Thus, this document will analyse the public data sources of infrastructure and buildings to be used at an urban parcel scale and determine the vulnerability of a large area such as the municipality of Ponferrada.

2 Study area

The study area, the municipality of Ponferrada, is located in northwest Spain (Fig. 1). The total vicinity has approximately 67,000 inhabitants, and it is the head of the region called El Bierzo (in the province of León, northwest of Spain). To understand the proposed analytical method, it is important to note that Ponferrada is divided into 6 districts and 45 census sections (Fig. 2) because not all of the available data used in this study were at the urban parcel scale.

The Sil River is the main water course in the area and meets two tributaries in the middle of the city. The overall drainage network has flooded the town several times. This is partly the reason for building three dams upstream of the town, together with agricultural water demands. The first dam is in the Boeza tributary with 2 hm³ of storage capacity, and it is out of the scope of the present study. The other two dams, Bárcena (341.5 hm³) and Fuente del Azufre (4 hm³), are in the Sil River. The present contribution focuses on evaluating the physical vulnerability of the town in the potential scenario that both dams break when they are at their maximum storage capacity. This scenario could have different origins. The first one would be for hydrological reasons. Bárcena is a loose material dam, and this type of dam presents a higher probability of breaking due to erosion of the protective coating when the crest is overtopped (Comité Nacional Español de Grandes Presas 2016). Another possible origin of the dam break would be structural failure. For this reason, the hydrological administration performs regular controls. Despite this oversight, some recent dam failures, such as those at Derna (Libya) and Braskereidfoss (Norway) in 2023, have raised the possibility that ageing is affecting dams beyond their economic and physical design life (Ho et al. 2017). One additional origin would be seismic activity (Ministerio de Medio Ambiente 2001). In this area, several faults cross along the Bárcena dam, associated with Cenozoic thrusts

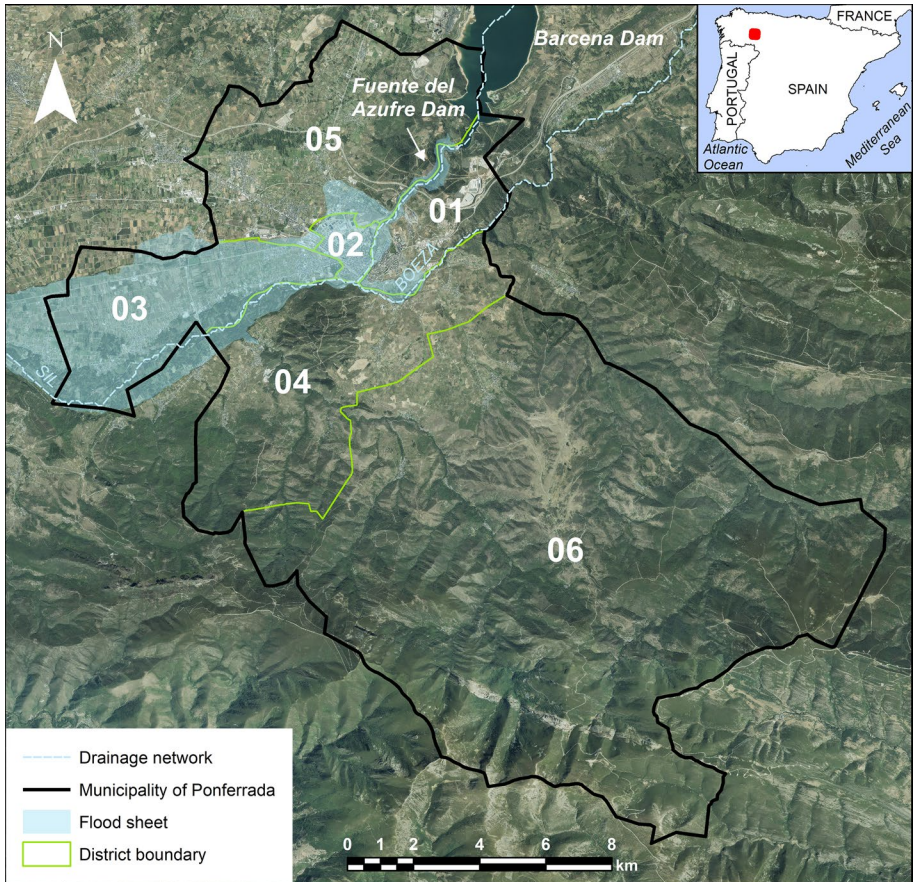


Fig. 1 Location of the study area with the simulated water sheet and the districts of the town (Image source: PNOA 2020)

(Martín-González and Heredia 2011a, 2011b), but they are categorized as low hazard according to the instrumental and historical records. These faults are associated with other structural and geomorphological features that played a role in the geomorphological development of the drainage pattern and the landscape configuration during Quaternary times (Mínguez 2015). Finally, there is the possibility of an anthropogenic origin, such as an act of terrorism.

The choice of this study area was reinforced by its geomorphological characteristics. As Fig. 1 shows, the town is located in the district 02, at the outlet of a confined reach of the Sil River, where the channel changes from a steep and narrow valley traversing more resistant igneous rocks, towards a wide area with friable sedimentary lithologies with a low slope. Without the dam, these areas are considered highly susceptible to floods. The geomorphological change from a narrow to a wide landscape lead to an expansion of the water sheet when floods occur. At the same time, the change in slope facilitates the runoff slowdown, which impedes water evacuation and increases flood damage. Therefore, considering the potential dam break and the location of the study area, the town presents a high flood hazard.

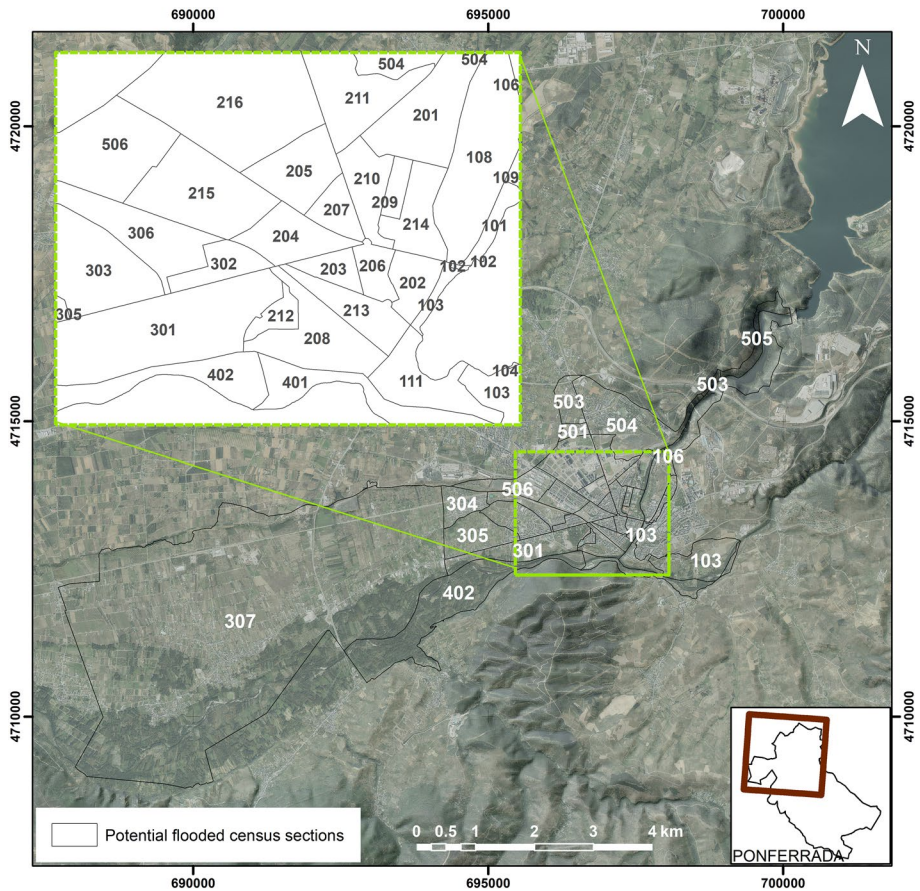


Fig. 2 Census sections in Ponferrada

However, not all of the town is at risk. Definition of the flood sheet extension was based on previous studies focused on the hydraulic modelling of the collapse of both dams (CHMiño-Sil 2012). Their results show an area inside the boundaries of the flood sheet where 45,338 inhabitants of the total 67,367 municipal inhabitants live (Tascón-González 2017). This affected area presents a wide range of modelled water height values. They move from the 85 m at the outlet of the confined river to the 25 m in the river downtown and the 15 m in the river at the south of the city.

3 Method and data sources

The methodological approach of using indicators to define the different factors that are involved in physical vulnerability allows comparison of the different building scenarios inside of a town or among towns. As in all types of vulnerability, the analysed factors may be classified into exposure and resistance. The factors associated with exposure reflect how an ecosystem is submitted to the effects of a natural event and its duration,

in this case a flood. Related to physical vulnerability, this ecosystem refers to infrastructure characteristics. On the other hand, the resistance factors show the capability of the society to protect itself, the capability of its immediate reaction and the capability to recover the former functioning of the society. These last factors may incorporate indicators related to land planning, such as the existence of floodplains allocated to alleviate peak discharge or the construction of artificial levees, river dikes or dams. At the end, both groups of factors relate to each other by Eq. 1 based on the method of Balica (2012):

$$PVI = (EL/R)/10 \quad (1)$$

where PVI is the physical vulnerability index, EL is the exposure level and R is the resistance. The final division by 10 is performed to achieve a PVI value inside the interval 0–1.

In the scientific literature it is observed that the most studied indicators are those referring to construction materials (Behazin et al. 2015; Krellenberg and Welz 2017; Fatemi et al. 2020), condition of the building (Thouret et al. 2014; Carlier et al. 2018; Xing et al. 2023), age building (Fernandez et al. 2016; Sadeghi-Pouya et al. 2017; Usman et al. 2021) and number of floors (Blanco-Vogt and Schanze 2014; Papathoma-Köhle et al. 2019; Leal et al. 2021). It should be noted that the determination of the construction materials indicator is carried out in study areas with a low number of buildings where it is relatively easy to carry out field work. This is performed through surveys where the damage suffered by the building is analyzed, depending on the material, once the flood has occurred. Unluckily, there is not a database with such information in the study area and the number of buildings is too large to get this type of data through a survey. Therefore, this paper does not include this indicator, although to get this type of data is strongly recommended for smaller areas.

The present method proposes an analysis divided into the following four steps:

- (1) Calculation of the different indicators. For the exposure level, the studied indicators are building age, percentage of the building affected by the flood based on the water height and percentage of harmed roads. For the resistance level, the researched indicators are the number of construction defences, the number of floodplains allocated to reduce downstream floods and the existence of land planning or emergency plans.
- (2) Normalization of each indicator. Each indicator has been converted to a scale of 0–1 to be able to combine and compare all of them without considering their different nature. In the case of exposure indicators, the value 1 means the highest vulnerability or the weakest infrastructure or building. The resistance indicators follow the inverse correlation. Two mathematical methods are used to normalize the data:
 - The correlation of percentages, by dividing the real value by 100. This method is applied in those indicators where data is in percentage.
 - The increasing linear function with a positive slope, which is applied to the rest of the indicators since their values are proportional to the degree of exposure or resistance. The normalized values will be calculated following the Eq. 2:

$$y = ((x - \text{Min})/((\text{Max} - \text{Min}))) \quad (2)$$

where y is the normalized value, x is the indicator value and min and max are the minimum and maximum potential limits of the indicator scale: a value lower or equal than the minimum will correspond to 0 and a value equal or higher than the maximum will correspond to 1.

- (3) Estimation of physical vulnerability exposure and resistance based on indicator weights. These weight values were the result of an Analytic Hierarchic Process (AHP) analysis carried out by Tascón-González (2017), in which she sent a survey to an expert panel comprising researchers, engineers and civil protection agents. Finally, she worked with 15 surveys that showed high consistency in the answers.
- (4) Application of Eq. 1 to calculate the physical vulnerability index.

In the following subsections, the first two steps are described for each chosen indicator. The two last steps are described together at the end of the section (Fig. 3).

3.1 Exposure indicator 1: building age

Buildings have evolved throughout history because of lifestyle changes and technological development. Modern buildings have adapted to the complex combination of social, cultural and productive dynamics. Therefore, there are significant changes between the old and the more recent buildings, with the oldest buildings being more vulnerable.

To estimate the real value of this indicator, the required input data came from cadastre or land registry administration. In Spain, this administration maintains an inventory of physical details pertaining to cadastral parcels, including their surfaces, locations, uses, shapes, cartographic representations, as well as information on the type and quality of constructions, among other factors (Cadastral Electronic Site 2023). These records adhere to the guidelines of the European Directive INSPIRE/Directive 2007/2/EC, Infrastructure for Spatial Information in Europe. The data is organized into three distinct datasets (Directorate General for Cadastre 2016). The first dataset focuses on cadastral parcels, which represent individual areas of land with uniform property rights and unique ownership. It contains the geometric information that outlines the boundaries of cadastral parcels in

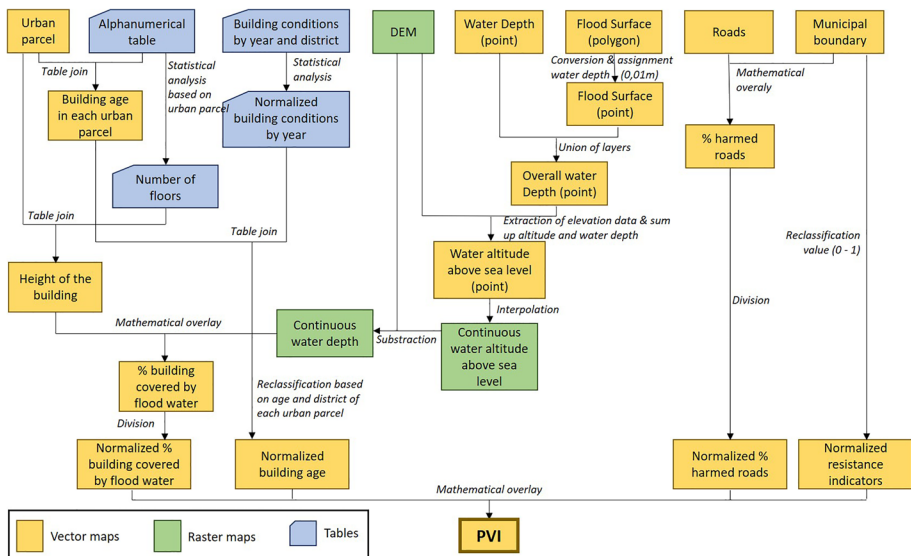


Fig. 3 Flow chart of the proposed method

both rural and urban areas. In this study, the urban polygons are also referred to as urban parcels indistinctively. The spatial resolution of the urban map is 1:1000 or higher. The second dataset stores the addresses and provides the location of properties based on identifiers such as street names and numbers, cities, and more. Therefore, this dataset primarily consists of attribute data rather than geographical information. Finally, the third dataset is dedicated to buildings and comprises geographical data that represent the geometry of the footprint of the buildings, along with a set of attributes stored in tabular format. All this information is currently available as open-source data.

Consequently, the vector map of the urban parcels and the alphanumeric table related to the building age were free downloaded to estimate the building age indicator. There was no problem to join both data in a Geographical Information System (GIS) because there was a unique correspondence between the buildings and the cadastre parcels, so the real value of building age was easily mapped (Fig. 4).

The second step, the normalization, included data related to building conditions for residential use: ruinous, bad, deficient and good. The proposed method related each term with a different normalization value (Table 1).

The first problem arising was that these data were distributed by districts, not by cadastre parcels. Hence, there were data on the percentage of buildings in a district that were in ruinous, bad, deficient or good condition for each year of construction (Table 2). The normalization of these data was achieved after calculating a weight mean of the Table 1 normalized values for each district and year (Table 2). Based on the year of construction of each urban parcel, these normalized values were assigned to each cadastral unit. This means that all parcels that were built during the same year in a district presented the same normalized value (Fig. 5).

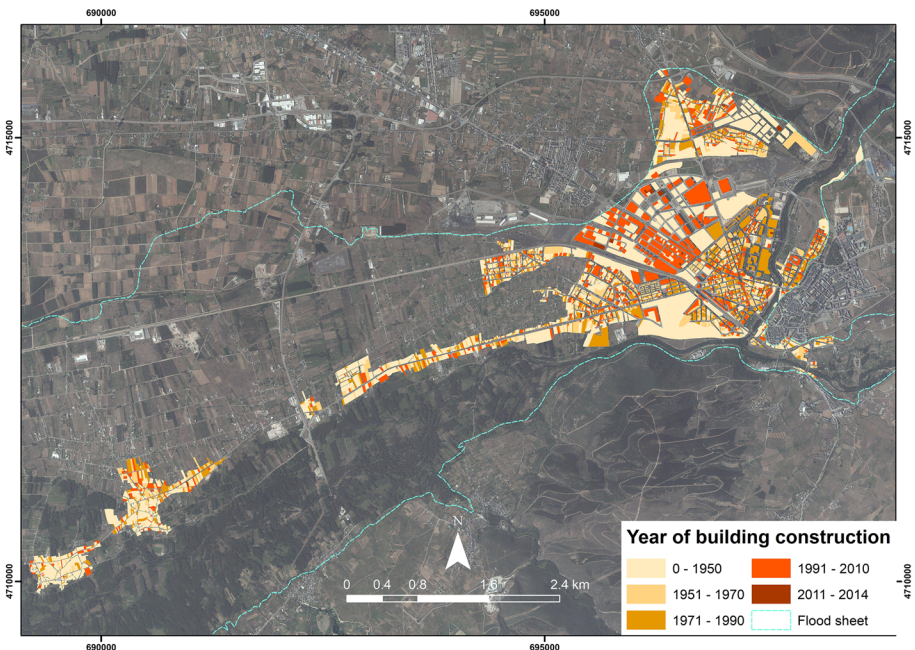


Fig. 4 Map of building construction year

Table 1 Normalized values for building conditions for residential use

Building condition	Normalized value
Ruinous	1
Bad	0.66
Deficient	0.33
Good	0

Table 2 Example of the Spanish national statistical institute database related to building conditions

District	Year of construction	Building condition	% of buildings	Normalized value for each parcel of the district
1	1965	Ruinous	15	$0.15 + 0.66 * 0.3 + 0.33 * 0.3 = 0.447$
		Bad	30	
		Deficient	30	
		Good	25	

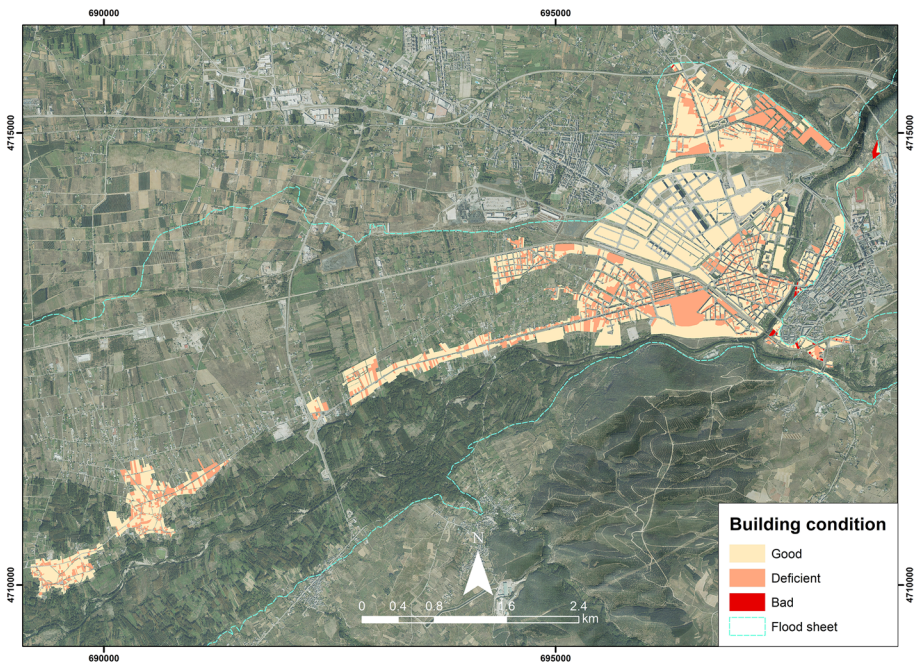


Fig. 5 Normalized value map of building conditions

The second problem was that there are only data about building conditions in residential parcels. The other areas aimed at commercial or industrial use did not show this type of data. The authors assumed that the situation of residential buildings was

common to the rest of the buildings, so the same Table 2 was used to classify commercial and industrial constructions.

3.2 Exposure indicator 2: building percentage covered by water

The objective of this indicator is to estimate the percentage of the building affected by the water depth. This means that at the same spatial coordinates, the lower the building height, the higher the physical vulnerability. To estimate the real value of this indicator, we divided the work into three parts. The first was to define the height of the buildings, differentiating those floors that were above and under the ground. The second was to estimate the water depth reached at each building. Finally, the percentage of the total building covered by the flood was calculated.

Again, part of the input data was acquired from the cadastre administration: the same polygon map with all the urban parcels that was used for building age indicator and another alphanumerical table. In this case, a digital elevation model (5 m×5 m), a polygon layer with the modelled water surface covered by the flood and a layer with 53 points with the modelled water depth value were also used.

The data needed to calculate the number of floors belonging to each building—above and under the ground—were available in the alpha numerical table. Each floor above the ground appeared in the alphanumeric table as positive values (1 for the first floor, 2 for the second, etc.). This means that several registers of the table corresponded to a unique building, one register per floor. Therefore, a new table was created with two fields: one corresponding to the urban parcel number (named as *Refcat*) and the other corresponding to the maximum value of the floors of each urban parcel. Something similar happened with the floors under the ground, but they appeared as negative values. The process was repeated, and a new field with the minimum value per parcel polygon was added to the recently created table. According to Ponferrada local urban norms, each floor has a 2.5 m vertical distance between the ceiling and the ground. A half metre was added considering the construction materials needed between the two consecutive floors. As a result, the height of the building was calculated by multiplying the number of floors above and under the ground by 3 m (Table 3, Fig. 6).

The next step was the estimation of the water flood depth in each building. In this case, as in many studies, there was a map with the flood extent, but there was not a continuum map with the water depth data (de Moel et al. 2009). Only 53 points with

Table 3 Example of some records in the new table with heights above and under the ground per building. The *Refcat* field corresponds to the urban parcel number

Refcat	Under floors	Above floors	Under metres	Above metres	Height of building (m)
7036905PH9173N	−4	6	12	18	30
5832331PH9153S	−2	7	6	15	21
001700600PH91F	0	1	0	3	3
0205101PH9100N	0	1	0	3	3
8140922PH9184S	−1	8	3	21	24
6033410PH9163S	−3	8	9	15	24

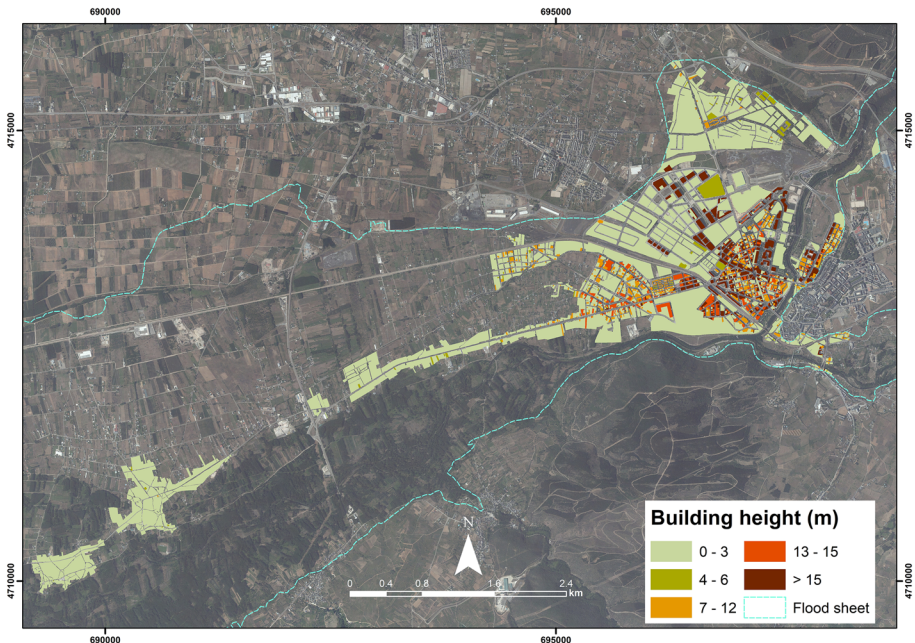


Fig. 6 Map of building heights (m)

estimated water depth and spread over the town were collected from the previous flood modelling study based on a potential dam break (CHMiño-Sil 2012). This number was integrated into the present work with those points corresponding to the flood extent perimeter modelled by the Water Administration. These last points conformed to the water limit, so it was considered that they had a minimum water depth (0.01 m). The values of water height at all the points were added to the terrain altitude extracted from the actual DEM, and afterwards, these water heights above sea level were interpolated by applying the natural neighbour kriging algorithm. The results showed a raster map with water altitudes above sea level. The last step consisted of subtracting the altitude values from the DEM. At this point, the distributed value of water height above the ground in the entire town was achieved (Fig. 7).

The goal of the following stage was to estimate the percentage of each building that was covered by the flood water. As an initial statement, it was considered that if a building with floors above ground was affected by the flood, the water also affected all of its underground floors. Consequently, the first step was to assign a water depth at each building. Based on statistical overlay analysis, the mean water height was assigned to each parcel of the cadastral vector map. Hence, this map had two types of data in its attribute table: the height of the building above the ground and the water depth. Next, a new field was created with the result of the building height minus the mean water height. If the result was negative or equal to zero, all of the building was affected, including those floors beneath the ground surface. If the result was positive, this meant that only part of the building was affected, although the underground floors were always considered affected. Based on these data, it was possible to estimate the percentage of the building covered by the flood water (Eq. 3) and to represent it through a map.

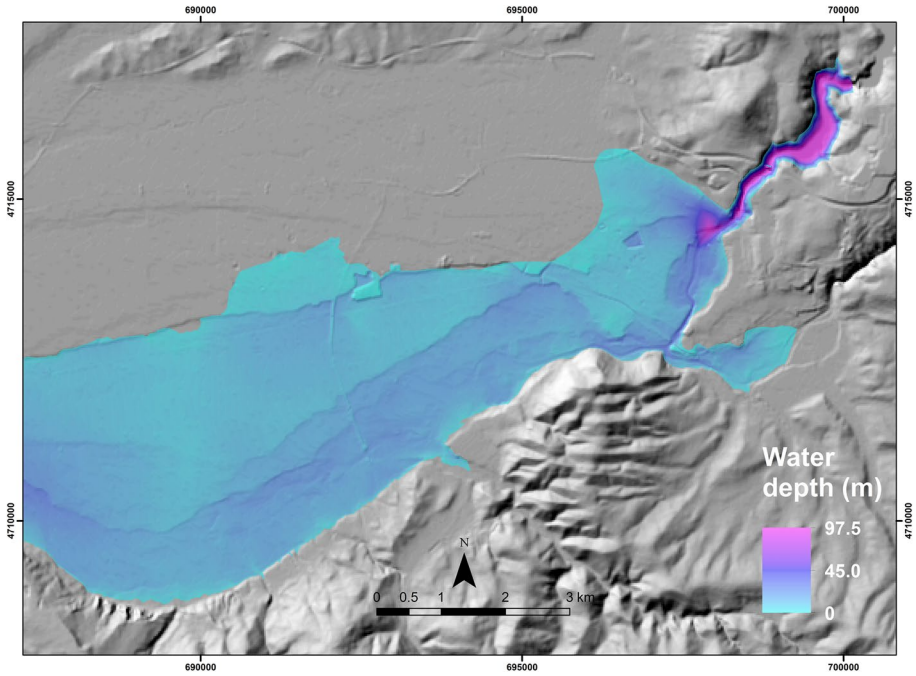


Fig. 7 Map of interpolated water depth (m)

$$\% \text{ building} = 1 - \frac{H_f}{H_b} * 100 \tag{3}$$

where H_f is the number of metres of the building free of flood water and H_b is the overall building height (including the underground floors).

To normalize this variable and to achieve a map with 0–1 values, it was only necessary to divide the pixel value by 100 (Fig. 8).

3.3 Exposure indicator 3: percentage of harmed roads

Physical vulnerability considers not only the building factor but also the infrastructure factor as the representation of the kind of services that allow regional development. This means that in flood areas, road safety implies flood risk management (Benedetto and Chia-vari 2010). Consequently, roads built in flood areas are more vulnerable to hazard impacts. For this reason, the indicator chosen to represent the transportation network vulnerability was the potential percentage of roads harmed by the flood.

This indicator distinguishes the number of road kilometres that are covered by the flood water surface compared to the number of road kilometres built in the study area. To estimate its real value, the following data sources have been consulted: the Spanish Works Ministry (Ministerio de Fomento 2017) and the image databases of World Imagery (2017) and World Street Map (2017). As can be inferred, the base unit of this analysis was the municipality, not the urban parcels. For the final study, the data set of the percentage of harmed roads at the

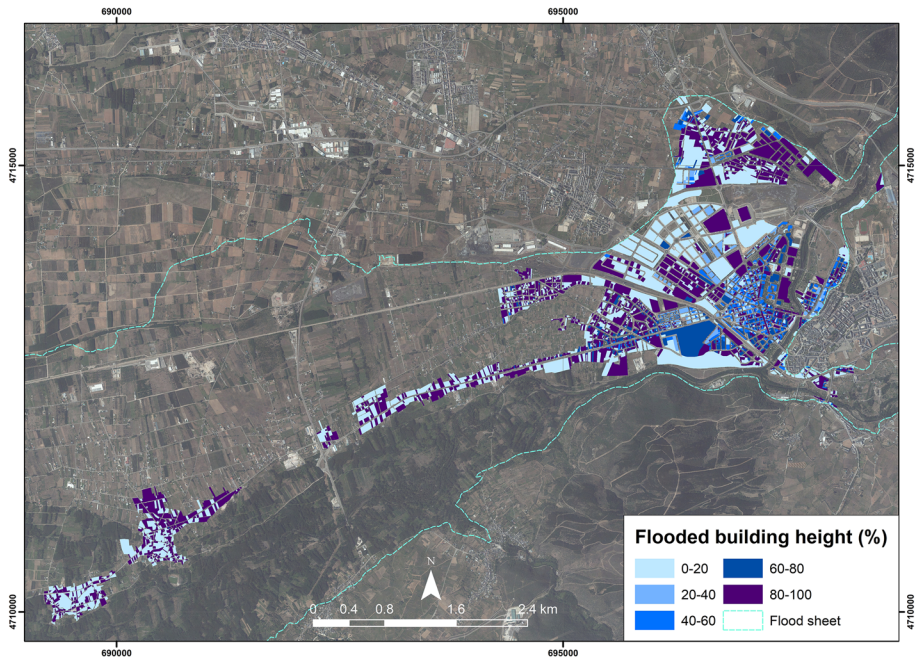


Fig. 8 Normalized value map of the building percentage covered by water

municipal level has been assigned at the urban parcel level, since the value of this indicator does not depend on the unit of analysis.

The easiest way to normalize this indicator represented by percentage is dividing the real value by 100, where values of 1 and 0 indicate the maximum and the minimum vulnerability, respectively (Tascón-González et al. 2020).

Finally, other infrastructure indicators were researched, such as telephone or electrical network, but none of them had free data available. For this reason, they were rejected from being incorporated in the present study. However, if available, it is strongly recommended to include them.

3.4 Resistance indicators

None resistance indicators were present in Ponferrada. There were no resistance measures that can minimize the effects of the flood wave if the dam breaks, especially if the dam size and proximity to the town are considered. Only previous land planning might assume flood resistance for buildings and infrastructures, and it did not exist in Ponferrada at the moment of the present study. For this reason, a minimum value of 0.1 was assigned as the normalized value, since division with value 0 would not be possible.

Table 4 Value assignment to indicators according to the AHP method (source: Tascón-González 2017)

ajk value	Interpretation	ajk value	Interpretation
1	j and k are equally important	1	j and k are equally important
3	j is slightly more important than k	1/3	j is slightly less important than k
5	j is more important than k	1/5	j is less important than k
7	j is much more important than k	1/7	j is considerably less important than k
9	j is absolutely more important than k	1/9	j is absolutely less important than k
2,4,6,8	Intermediate values	1/2,1/4,1/6,1/8	Intermediate values

Table 5 Example of values assigned by an expert applying the AHP method

	j	k	h
j	1	1/5	3
k		1	7
h			1

3.5 Physical vulnerability index

To estimate the PVI, the first step was to calculate the exposure level. For this purpose, different weights were assigned to each indicator (Table 4) following the AHP analysis (Tascón-González 2017).

The AHP method first considers a set of evaluation indicators and generates a weight for each of them according to the pairwise comparisons made by a panel of experts. As a result, the method supplies a pairwise comparison matrix, where the higher the weight, the more important the corresponding indicator is. In addition, the AHP method allows checking the consistency of the evaluations to reduce bias in the decision-making process. This is essential when many pairwise comparisons are carried out, as some inconsistencies may arise.

To develop the method, the respondent is asked to:

- (1) Order the indicators according to their importance (1 the most important) giving the same value to those that they consider equal.
- (2) Provide their opinion regarding the weight of the selected indicators, comparing them two by two in a table and assigning to each relationship the values detailed in Table 4.

where *j* and *k* are indicators and *ajk* represents the importance of the *j*th indicator relative to the *k*th indicator. To facilitate their assignment, an example is presented below in which the following indicators are compared (Table 5):

- *J* is the percentage of homes affected by the sheet of water considering the height at which they are located
- *ki* is the percentage of old and poorly maintained homes affected by the sheet of water
- *h* is the percentage of roads affected by the sheet of water

Based on the values assigned by all experts, it is possible to assign weights to each physical vulnerability indicator. The final weights are shown in Table 6.

Subsequently, the three indicator raster maps were mathematically overlaid with their corresponding weights and the result generated the flood exposure map of the physical vulnerability index.

The following step was to calculate the physical vulnerability index map. Based on Eq. 1, the exposure level should be divided by the resistance value, 0.1, after considering the low resistance that Ponferrada now shows concerning flood hazards without any planning. The division of the exposure value map by such a low resistance value map assumed that the PVI values were higher than the 0–1 range. Consequently, the results were divided by ten to normalize the PVI. For this reason, with this method, where the resistance value is almost null, the PVI map presents the same values as the exposure map.

4 The physical vulnerability map

The application of the previous method allowed the generation of the physical vulnerability map of Ponferrada where the closeness to the infrastructure breach has appeared as an aggravation of risk in several cases (Creach et al. 2016). At the same time, a distributed map of the PVI (Fig. 9) has been achieved. This index is grouped into 5 classes: very low, low, medium, high and very high considering the relationship of values between the degree of exposure and resistance (Müller et al. 2011; Baky et al. 2020). The analysis of the vulnerability data by districts shows their internal variability. The minimum value in all of the districts is 0.059. This value partly corresponds to those urban parcels without buildings, where the PVI value is due to the harmed road indicator of the overall municipality. For the following analysis, these parcels without buildings are out of scope. The rest of the parcels that show this low vulnerability value correspond with buildings located close to the water sheet perimeter, where water depth is so low that buildings are not affected by the flood.

Overall, of the 6441 studied urban parcels in Ponferrada, 261 parcels (4%) showed values higher than 0.5, which were considered very highly vulnerable. In addition, 1203 urban parcels (18.7%) were included in the interval 0.4–0.5, which was considered highly vulnerable. The rest of the parcels showed low values. The mean PVI value overall in the study area is 0.26, which is considered a medium–low value in terms of vulnerability.

From a district point of view, district number 4 presents the lowest PVI value (0.188). This district only has a census section affected by the flood, so its PVI values are quite homogenous. The maximum PVI values reached inside all of the districts are over 0.45 (Table 7). The only exception is district 4, where the maximum value is 0.378. This low minimum value matches the lowest average PVI value of the district. Another district with homogeneous PVI values is number 2. In this case, it is in the right margin of the river

Table 6 Indicator weights proposed to estimate the exposure level (Tascón-González 2017)

Indicators	Weight (w_i)
Building age	0.505
% of the building affected by the flood based on the water height	0.319
% of harmed roads	0.176

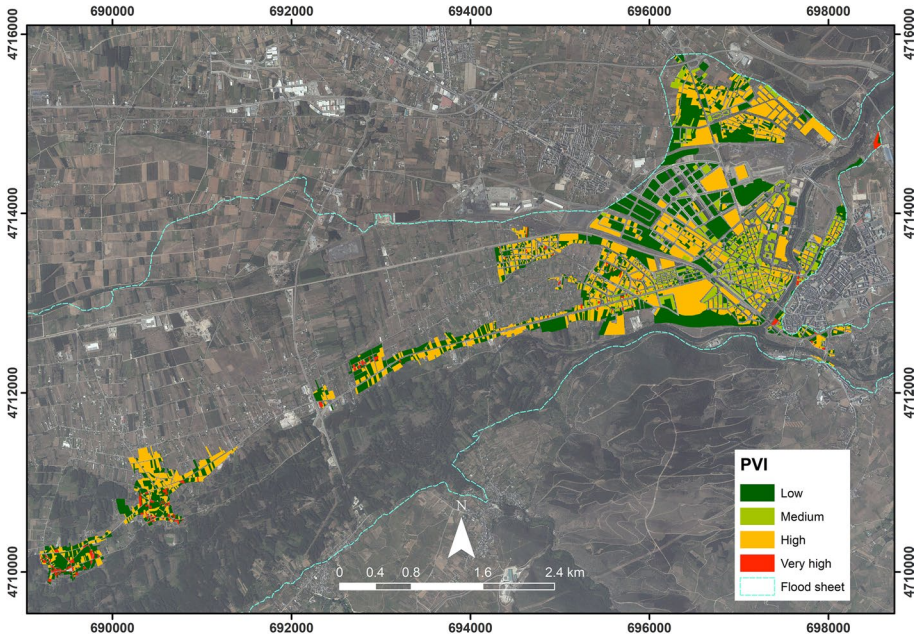


Fig. 9 Map of the physical vulnerability index

Table 7 Basic statistics of PVI values by district

District	Mean	Maximum	Minimum	Standard dev
1	0.253	0.563	0.059	1.50
2	0.280	0.489	0.059	1.36
3	0.253	0.545	0.059	1.71
4	0.188	0.378	0.059	1.36
5	0.269	0.469	0.059	1.59
Total	0.261	0.563	0.059	1.60

where the floodwater reaches the greatest depth in the census section number 214 (Table 8 and Fig. 10).

The rest of the districts show more heterogeneity in PVI values. District 1 corresponds to the old town area, partly located on a hill. These elevated areas may be affected by the flood but with low water depths. Nevertheless, other urban parcels in this district are at lower altitudes. This is the reason why some PVI values are higher than 0.5. Therefore, District 1 displays a wide range of PVI values. District 5 presents low PVI values in general. It is a district located close to the perimeter of the floodwater sheet, with relatively new buildings. The exception is Section 504, where water reaches a high-water depth together with bad building conditions. Finally, District 3 developed along the river with a low concentration of urban areas. It shows the highest internal PVI heterogeneity values because it is an extended district with some houses close to the river and others close to the perimeter of the floodwater sheet. The highest PVI values are reached in census Section 307, where there are many one-floor buildings in bad condition.

Table 8 Basic statistics of PVI values by census section

Census section	Mean	Maximum	Minimum	Standard dev
101	0.206	0.563	0.059	1.14
102	0.240	0.563	0.071	1.79
103	0.309	0.563	0.059	1.72
104	0.199	0.338	0.059	1.97
106	0.141	0.563	0.059	1.79
108	0.286	0.563	0.059	1.23
109	0.280	0.563	0.059	1.21
111	0.169	0.563	0.059	1.51
201	0.347	0.489	0.059	1.33
202	0.292	0.489	0.059	1.37
203	0.278	0.489	0.059	1.29
204	0.306	0.489	0.059	1.45
205	0.167	0.464	0.059	0.92
206	0.316	0.489	0.059	1.27
207	0.259	0.489	0.059	1.34
208	0.280	0.489	0.059	1.60
209	0.226	0.378	0.059	1.44
210	0.293	0.489	0.059	1.25
211	0.182	0.378	0.059	0.91
212	0.270	0.403	0.150	0.59
213	0.280	0.489	0.059	0.93
214	0.398	0.489	0.059	0.97
215	0.305	0.378	0.059	1.31
216	0.118	0.378	0.059	0.92
301	0.248	0.545	0.059	1.59
302	0.203	0.545	0.059	1.11
303	0.307	0.545	0.059	1.49
304	0.273	0.545	0.059	1.60
305	0.304	0.545	0.059	1.49
306	0.271	0.410	0.059	1.24
307	0.217	0.545	0.059	1.91
401	0.188	0.378	0.059	1.36
501	0.143	0.469	0.059	1.07
503	0.216	0.469	0.059	1.38
504	0.307	0.469	0.059	1.54
506	0.132	0.378	0.059	1.19
Total	0.261	0.563	0.059	1.600

All these PVI values are conditioned by the distribution of the different indicators. The most influential indicator in Ponferrada is the building percentage covered by water (Fig. 9). It is important to note that the largest water depth reaches 20.25 m in Ponferrada, so the number of buildings highly affected by an elevated water depth is high (Table 9). The comparison of these values with the building heights (Table 10) makes it easy to understand the high vulnerability of the urban parcels.

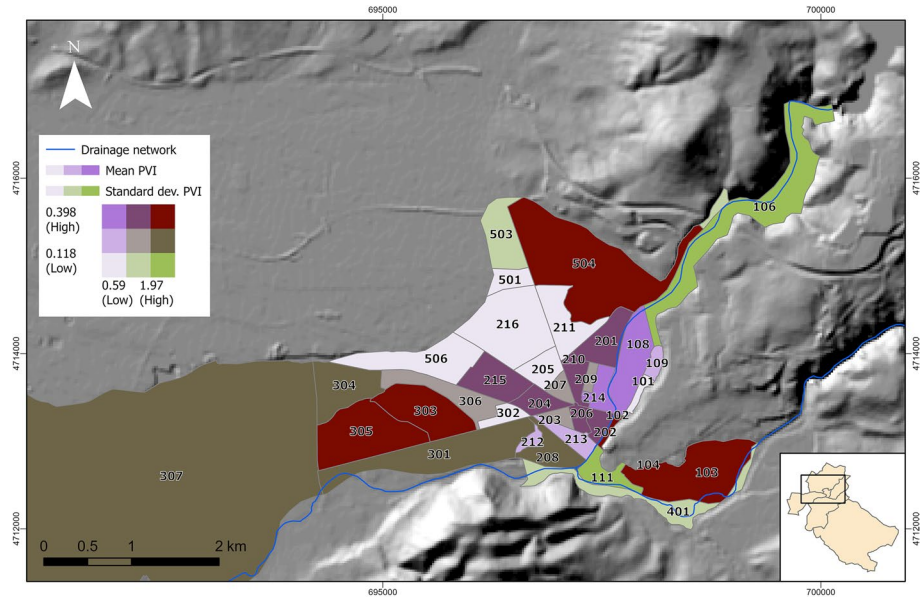


Fig. 10 Mean PVI values and their standard deviation distributed by census section

Table 9 Simulated water depths in the flood area

Water depth (m)	Number of buildings
0–1	152
1–3	280
3–6	1515
6–10	1608
> 10	1007

Table 10 Building heights

Number of building floors above terrain	Number of buildings
1	2873
2	105
3	265
4	454
> 4	865

Indeed, the main map (Fig. 9) shows many buildings (2786 urban parcels) affected 100% by the water depth. Again, those 1879 urban parcels without buildings appear with a 0-value indicator. The high level of vulnerability index present in the urban parcels located in district 3 is relevant because of the type of building. Most of them are one-floor

buildings, so although the water depths are not as high as in other districts, the floodwater easily covers the houses.

Despite the high importance of the water depth versus building height, the panel of experts gave their maximum weight value to the building condition indicator. The analysis of the results showed that 1810 buildings had the minimum value because of their good building condition. All of them were built after 1970 and are spread over all of the districts of the town. The highest exposure values with this indicator are in districts 3 and 5 and match with constructions built in the period 1900–1920 (Table 11). None of the other districts has buildings of this period.

A very small area of district 4 is affected by the flood. It is only a small part of the census Section 401, and it is not representative of the overall district. For this reason, assigning the building condition values of the district 4 in general would include errors. That is why the same building conditions of the neighbouring 103 census section were assigned to those buildings in Section 401.

The general good building conditions, regardless of age, are responsible for not reaching the maximum potential vulnerability value in the final map.

In the case of harmed roads, the importance of this indicator in the analysis is very low due to the low number of affected kilometres and the low AHP weight value. From the 884 km of roads that are in the municipality, only 292 km would be harmed by the flood. This represents 33% of the total studied roads.

5 Discussion

At this moment, the open-access data available in several countries allow an improve in the analysis scale without an increase in time and money. Ten years ago, this study would have presented just a unique indicators' value for the entire municipality. Instead, the new studies may show the spatial variability of the indicators inside the municipality, and it is possible to differentiate the flood vulnerability of each urban parcel. Therefore, they are basic to increasing societal security and improve the decision-making process (Abdelrahman 2021). For instance, in the studied case of a dam break, a large area will be flooded due to its proximity to the dam, but different risk degrees have been detected. As a result, the re-use of the open-access data for specific applications like the one presented in this study supports that these data create value for the society and its economic development (Cowan et al. 2014). In cases where cadastral mapping is unavailable in the study area, an alternative approach for generating a vector map with urban parcels is through satellite image segmentation (Chhor et al. 2017; Feng et al. 2020). So, parcels will be distinguished according to their different type of the rooftops. However, when utilizing this method, detailed information such as building age, number of floors, and other characteristics may not be attainable. Then, conducting a survey among the local population would be the only viable option to gather comprehensive data on these aspects. But this option only is possible when the towns are small.

Overlaying maps of different scales can introduce inconsistencies and inaccuracies into the results (Bailey 1988 and Chrisman 1987). In this study different map scales with different elementary units, such as the urban parcel, the census section, the district area, the municipality and the 5 m × 5 m pixel, were used (Table 12). The choice of the unit type for each variable was made based on the intrinsic nature of the indicator. For example, the number of road km does not make sense by urban parcel, it is a variable

Table 11 Number of buildings according to their building condition and district (source: INE 2011)

Construction year	Building condition	Number of buildings			
		District 1	District 2	District 3	District 5
1900–1920	Total	–	–	160	105
	Bad	–	–	–	35
	Deficient	–	–	160	60
	Good	–	–	–	10
1921–1940	Total	100*	–	35*	60
	Bad	25	–	–	–
	Deficient	55	–	10*	50
	Good	15	–	25*	10
1941–1950	Total	260	495	290	340
	Ruinous	30	–	–	–
	Bad	40	70	–	15
	Deficient	115	100	55	150
	Good	75	325	235	175
1951–1960	Total	680	1770	1380*	550*
	Ruinous	20	15	–	–
	Bad	40	10	–	25
	Deficient	50	200	195	145
	Good	570	1545	1190	375
1961–1970	Total	1315	2335	1290	740
	Bad	–	–	–	10
	Deficient	45	60	95	85
	Good	1270	2275	1195	645
1971–1980	Total	2175	2335	1135	710*
	Deficient	–	60	45	20
	Good	2175	2275	1090	685
1981–1990	Total	1620	2425	795*	960
	Bad	–	–	–	15
	Deficient	–	–	20*	–
	Good	1620	2425	770	945
1991–2001	Total	2465	2850	1040	1285
	Good	2465	2850	1040	1285
2002–2011	Total	1265	2225	830	655
	Good	1265	2225	20	655

*This means that the value is an approximation

for the overall municipality. Nevertheless, the overlay of these layers does not involve any inconsistency nor inaccuracy since the polygons of the larger scale are completely inside of one polygon of the layer with smaller scale. There cannot be an urban parcel between two census section nor two census section between two municipalities. In this way, the information of the smallest scale has been extracted towards the spatial units of the largest scale layer (the cadastre parcel). Furthermore, adopting the urban parcel as

Table 12 Elementary units used in the index analysis

	Indicators and index	Variable	Elementary unit
Input	Building age	Building construction year	Cadastre parcel
		Building condition	District area
	Building percentage covered by water	Height of the buildings	Cadastre parcel
		Water depth	5 m × 5 m pixel
	Percentage of harmed roads	Number of road km	Municipality
Output	Physical vulnerability index		Cadastre parcel Census section

the unit of analysis for most indicators enables the application of this method in towns of any scale, enhancing the adaptability and versatility of the proposed methodology.

Another advantage of the proposed method is that the results may help to define the emergency planning of the town. Water might reach the town of Ponferrada in a very short time (15 min). In case that some citizens cannot reach out the water perimeter, the index maps can become a useful tool to identify those buildings located inside the water sheet that fulfil saved characteristics as meeting points. Therefore, this type of analysis represents a good improve in the flood planning for those scenarios originated by rainfall or snow melting. But the emergency planning might present some problems when trying to define meeting points in buildings when floods come from a dam break. In this case, it is not possible to model the exact behaviour of the building structures when the water wave reaches them. This means that some of them might fall because of the water impact, although other buildings that are located inside the flood extent map might remain safe in the uppermost floors. The uncertainties of engineering studies in this aspect are still very high (Paquier and Goutal 2016). For this reason, it is necessary to improve the wave impact and sediment transport modelling before buildings inside the flood area are designated as meeting points. Despite the presence of these uncertainties, the awareness of their existence may facilitate the design of a flexible emergency planning to anticipate and adjust to future changes. This approach is consistent with the resilience-enhancing strategies supported by Berkes (2007).

At the same time, there are other uncertainties related to the number of citizens at each urban parcel that would help to better define the meeting points. In this case, the data exists, but the present Spanish legislation does not allow its use out of the Administration's studies. Despite all the advantages, the use of open data may lead to claims for individual rights due to conflict with the personal data protection laws. So, while everybody defends that public data belong to the citizens, it is important that the access to these governmental data follows a legal framework to guarantee everybody's rights (Abdelrahman 2021). Otherwise, identity can be inferred from data and the privacy of individuals can be affected (Cowan et al. 2014). Anyhow, although these uncertainties, the proposed PVI analysis based on cadastre parcels represents an important new data source to be included in emergency planning.

The time interval between flood hydraulic modelling and emergency planning may lead to other inconsistencies, in this case related to altitude data. The introduction of LiDAR data in altitude mapping in recent years has improved the accuracy of height data but has resulted in problems when combining with older data. For this reason, it is necessary to adapt the water levels of former modelling to LiDAR altitudes, considering the perimeter points of the water sheet extension. Again, GIS is an extremely helpful tool in this process and allows mapping the percentage of each building that is covered by the floodwater. With

this method, water depth is considered spatially variable and diminishes the overestimations of a unique water depth value in the entire town, as noted by Breilh et al. (2013). Nevertheless, this spatial analysis would have been avoided if data from the previous dam-break study would have been open-accessed and instead of few points with water height data the complete modelled raster map would have been left as open-access data. It is what Abdelrahman (2021) calls prevalence of closed government culture and lack of open government data policy. Reports of this type of studies are often available after requesting personally for them, but the Administration is reticent to give spatial data of this kind, maybe due to fear to data misinterpretation and misuse (Zuiderwijk and Janssen 2014).

The building condition map is another tool to help diminish the vulnerability of a society. The objective of this variable is to consider the potential of roof collapses, wall failures or foundations undermined, all of which are part of the building elements most often damaged by a flood (Kelman and Spence 2004). Although the open government data do not offer extensive details about building conditions, cross referencing with other data related to the age of the infrastructure (or the age of the last extension or rehabilitation of the building) allows improvement of building characteristics. It also provides a first global view of the building capability of resistance. In the case of Ponferrada, this factor is the critical when analysing the town's resilience. The majority of the buildings shows good conditions which enhances their resistance when facing the water wave generated by the potential dam break. The main issues are concentrated in districts 3 and 5, located downtown, in the oldest area of the city. Nevertheless, some of these buildings may have undergone various types of internal rehabilitation (not recorded by the Cadastre Administration) that could have affected their structural integrity. In this case, the concept of data collaboratives would represent a benefit for citizens (Susha et al. 2019), considering the insurance companies as the collaborative entities. Sanderson et al. (2022) remarked the importance of the interactions among different entities to improve resilience planning. The incorporation of this collaborative data could facilitate the implementation of local policies focused on improving the resistance of the building materials or the urban planning to relocate potentially affected population in the event of flooding, among others. As a consequence, this investment would help to reach some of the 4 R's of resilience (Kameshwar et al. 2019): *robustness* (ability to absorb damage) and *rapidity* (ability to rapidly recover). While there is enough data about building conditions in the national open-access database, there is a lack of available data related to infrastructures. The physical vulnerability map of this study only includes roads. Other infrastructure networks, such as electricity, water, telecommunications and internet, should also be included in future studies to improve the physical vulnerability results. At this moment, almost without exception, societies are highly dependent on these infrastructures for their current way of life. They are critical infrastructures, and without them, the goods and services that protect life would be at risk. This type of data faces two problems. The first is that most of these data belong to private enterprises, so their access is difficult to achieve. Data exchange among companies and government is still difficult due to legal barriers related to proprietary nature of data (Susha et al. 2019). The second is the lack of methodology to establish indicators that represent the vulnerability of these variables. Until now, few studies have focused on estimating the damage after the event has occurred (Dall'Osso et al. 2009; Guillard-Goncalves 2016; Azmeri and Isa 2018). Although these difficulties for working with infrastructure data, we consider that their inclusion in future PVI will represent an important improve in the vulnerability evaluation of the society.

This study has focused on physical vulnerability. However, the analysis of social and economic factors is fundamental to enhance the resilience of the society, where disaster data such

as the inclusion of rescue, evacuation or hospitalization operations during and immediately after the flood event might be included (Lin et al. 2017).

6 Conclusion

The proposed method has shown a high adaptability and versatility to data sources with different units of analysis after being tested in a medium-sized population. At the same time, the spatial analysis has once again showed being a powerful tool to estimate the flood vulnerability, displaying the geographical diversification of each indicator and the final PVI. Of all indicators, the most relevant ones have been, firstly, the percentage of affected buildings based on the depth and, secondly, the age of the buildings. The AHP approach to define the weight of each indicator gives excellent results, in case besides the weight matrix the evaluators add an ordered list of the indicators according to their importance. The overall resulting maps represent an important progress when developing prevention programs, as well as emergency and evacuation plans, by delimiting the most vulnerable areas and pointing potential meeting points to increase the resilience against floods. Future local policies should focus in these areas to achieve a resilient society, improving the quality of the buildings and developing new urban planning to avoid increasing the population on them. However, none of these measures should be considered without combining the results of the present study with a socio-economic approach to the vulnerability of Ponferrada.

On the other hand, in this paper, we have argued that the new open-access data facilitates the estimation of the physical vulnerability index in flood risk analysis from a potential dam break. Nevertheless, though these new open sources have increased the amount of available data for this type of studies, there is still a lack of data related to material construction and the infrastructure networks considered critical for the present standard way of life. Efforts should be focused in the following years on making open access this type of data that is currently in private hands. The access to these data should follow a legal framework to guarantee everybody's rights, but, at least, it is necessary to share this cartography with the local administration. In this way, risk analysis studies ordered by municipalities will be able to include other indicators related to infrastructure, such as telephone, electricity or water networks, improving the resilience of the society and decreasing the vulnerability.

Author contributions All authors have read and agreed to the published version of the manuscript. Conceptualization, EGM. and MFJ; methodology, all authors.; data collection and material preparation, LTG.; GIS analysis, LTG and MFJ; writing—original draft preparation, LTG; writing—review and editing, all authors.

Funding Open Access funding provided thanks to the CRUE-CSIC agreement with Springer Nature. This research was funded by the Spanish Ministry of Science, Innovation and Universities, grant ESP2017-89045-R, and by Junta de Castilla y León, grant LE169G18.

Declarations

Conflict of interest The authors have no relevant financial or non-financial interests to disclose.

Open Access This article is licensed under a Creative Commons Attribution 4.0 International License, which permits use, sharing, adaptation, distribution and reproduction in any medium or format, as long as you give appropriate credit to the original author(s) and the source, provide a link to the Creative Commons licence, and indicate if changes were made. The images or other third party material in this article are included in the article's Creative Commons licence, unless indicated otherwise in a credit line to the material. If material is not included in the article's Creative Commons licence and your intended use is not

permitted by statutory regulation or exceeds the permitted use, you will need to obtain permission directly from the copyright holder. To view a copy of this licence, visit <http://creativecommons.org/licenses/by/4.0/>.

References

- Abdelrahman OH (2021) Open Government Data: development, practice, and challenges. In: Kakulapati V (ed) Open data, intechopen. <https://doi.org/10.5772/intechopen.100465>
- Adger WN (2000) Social and ecological resilience: are they related? *Prog Hum Geogr* 24:347–364. <https://doi.org/10.1191/030913200701540465>
- Aksha S, Juran L, Resler LM, Zhang Y (2019) An analysis of social vulnerability to natural hazards in Nepal using a modified social vulnerability index. *Disaster Risk Science* 10:103–116. <https://doi.org/10.1007/s13753-018-0192-7>
- Aroca E, Bodoque JM, García JA, Díez A (2017) Construction of an integrated social vulnerability index in urban areas prone to flash flooding. *Nat Hazard* 17:1541–1557. <https://doi.org/10.5194/nhess-17-1541-2017>
- Azmeri A, Isa AH (2018) An analysis of physical vulnerability to flash floods in the small mountainous watershed of Aceh Besar regency, Aceh province, Indonesia. *Jamba: J Disaster Risk Stud* 10(1):550. <https://doi.org/10.4102/jamba.v10i1.550>
- Bailey RG (1988) Problems with using overlay mapping for planning and their implications for geographic information systems. *Environ Manag* 12(1):11–17. <https://doi.org/10.1007/BF01867373.pdf>
- Baky MAA, Islam M, Paul S (2020) Flood hazard, vulnerability and risk assessment for different land use classes using a flow model. *Earth Syst Environ* 4:225–244. <https://doi.org/10.1007/s41748-019-00141-w>
- Balica SF, Douben N, Wright NG (2009) Flood vulnerability indices at varying spatial scales. *Water Sci Technol* 60(10):2571–2580. <https://doi.org/10.2166/wst.2009.183>
- Balica SF (2012) Applying the flood vulnerability index as a knowledge base for flood risk assessment (Unpublished PhD Thesis). Delft University of Technology and the Academic Board of the UNESCO-IHE. Institute for Water Education
- Behanzin ID, Thiel M, Szarzynski J, Boko M (2015) GIS-based mapping of flood vulnerability and risk in the Bénin Niger river valley. *Int J Geomat Geosci* 6:1653–1669
- Benedetto A, Chiavari A (2010) Flood risk: a new approach for roads vulnerability assessment. *WSEAS Trans Environ Dev* 6(6):457–467
- Berkes F (2007) Understanding uncertainty and reducing vulnerability: lessons from resilience thinking. *Nat Hazard* 41:283–295. <https://doi.org/10.1007/s11069-006-9036-7>
- Bigi V, Comino E, Fontana M, Pezzoli A, Rosso M (2021) Flood vulnerability analysis in urban context: a socioeconomic sub-indicators overview. *Climate* 9(1):12. <https://doi.org/10.3390/cli9010012>
- Bisbal A, Picón J, Casaverde M, Jáuregui F, Anchayhua R, Masana M (2006) Manual básico para la estimación del riesgo. Instituto nacional de defensa civil. Lima-Perú
- Blanco-Vogt A, Schanze J (2014) Assessment of the physical flood susceptibility of buildings on a large scale—conceptual and methodological frameworks. *Nat Hazard* 14:2105–2117. <https://doi.org/10.5194/nhess-14-2105-2014>
- Breilh JF, Chaumillon E, Bertin X, Gravelle M (2013) Assessment of static flood modeling techniques: application to contrasting marshes flooded during Xynthia (western France). *Nat Hazards Earth Syst Sci* 13(6):1595–1612. <https://doi.org/10.5194/nhess-13-1595-2013>
- Cadastral Electronic Site (2023) Help for Cadastral Electronic Site (SEC). https://www.catastro.meh.es/ayuda/english_ovc.htm
- Carlier B, Puissant A, Dujarric C, Arnaud-Fassetta G (2018) Upgrading of an index-oriented methodology for consequence analysis of natural hazards: application to the upper guil catchment (southern French Alps). *Nat Hazard* 18:2221–2239. <https://doi.org/10.5194/nhess-18-2221-2018>
- Cheng H, Chen Z, Huang Y (2022) Quantitative physical model of vulnerability of buildings to urban flow slides in construction solid waste landfills: a case study of the 2015 Shenzhen flow slide. *Nat Hazards* 112:1567–1587. <https://doi.org/10.1007/s11069-022-05239-5>
- Chhor G, Aramburu CB, Bougdal-Lambert I (2017) Satellite image segmentation for building detection using U-Net. <http://cs229.stanford.edu/proj2017/final-reports/5243715.pdf>
- CHMIÑO-SIL-Confederación Hidrográfica del Miño-Sil (2012) Plan de emergencia de la presa de Bárcena. Non-published document
- Chrisman NR (1987) The accuracy of map overlays: a reassessment. *Landsc Urban Plan* 14:427–739. [https://doi.org/10.1016/0169-2046\(87\)90054-5](https://doi.org/10.1016/0169-2046(87)90054-5)

- Comité Nacional Español de Grandes Presas (2016). Guías técnica de seguridad de presas n° 2. Criterios para proyectos de presas y sus obras anejas (Tomo II). Presas de materiales sueltos. Comité Nacional Español de Grandes Presas. 198 pp
- Cowan D, Alencar P, McGarry F (2014) Perspectives on open data: issues and opportunities. In: IEEE international conference on software science, technology and engineering. Ramat Gan, Israel, pp 24–33. <https://doi.org/10.1109/SWSTE.2014.18>
- Creach A, Chevillat-Miot E, Mercier D, Pourinet L (2016) Vulnerability to coastal flood hazard of residential buildings on Noirmoutier island (France). *J Maps* 12(2):371–381. <https://doi.org/10.1080/17445647.2015.1027041>
- Dall’Osso F, Gonella M, Gabbianelli G, Withycombe G, Dominey-Howes D (2009) Assessing the vulnerability of buildings to tsunamis in Sydney. *Nat Hazards Earth Syst Sci* 9:2015–2026
- De Loyola H, Cutter SL, Emrich CT (2016) Social vulnerability to natural hazards in Brazil. *Int J Disaster Risk Sci* 7:111–122. <https://doi.org/10.1007/s13753-016-0090-9>
- De Moel H, Van Alphen J, Aerts CJH (2009) Floods maps in Europe—methods, availability and use. *Nat Hazard* 9:289–301. <https://doi.org/10.5194/nhess-9-289-2009>
- Directorate General for Cadastre (2016) Inspire dataset of the Directorate General for Cadastre: Cadastral Parcels (CP), Addresses (AD) and Buildings (BU), version 1.0. https://www.catastro.minhap.es/webinpire/documentos/Conjuntos%20de%20datos_en.pdf
- Dunning CM, Durden S (2013) Social vulnerability analysis: a comparison of tools. Institute for Water Resources, p 34
- Erena SH, Worku H (2019) Urban flood vulnerability assessments: the case of Dire Dawa city, Ethiopia. *Nat Hazards* 97:495–516. <https://doi.org/10.1007/s11069-019-03654-9>
- Ezell BC (2007) Infrastructure vulnerability assessment model (I-VAM). *Risk Anal* 27:571–583. <https://doi.org/10.1111/j.1539-6924.2007.00907.x>
- FEMA (2011) Buildings and infrastructure protection series. Reference manual to mitigate potential terrorist attacks against buildings. FEMA
- Feng W, Sui H, Hua L, Xu C, Ma G, Huang W (2020) Building extraction from VHR remote sensing imagery by combining an improved deep convolutional encoder-decoder architecture and historical land use vector map. *Int J Remote Sens* 41:6595–6617. <https://doi.org/10.1080/01431161.2020.1742944>
- Fernandez P, Mourato S, Moreira M, Pereira L (2016) A new approach for computing a flood vulnerability index using cluster analysis. *Phys Chem Earth* 94:47–55. <https://doi.org/10.1016/j.pce.2016.04.003>
- Fuchs S, Heiss K, Hübl J (2007) Towards an empirical vulnerability function for use in debris flow risk assessment. *Nat Hazard* 7:495–506. <https://doi.org/10.5194/nhess-7-495-2007>
- Gaillard JC, Texier P (2010) Religions, natural hazards, and disasters: an Introduction. *Religion* 40(2):81–84. <https://doi.org/10.1016/j.religion.2009.12.001>
- Gallopin GC (1997) Indicators and their use: information for decision-making. In: Moldan B, Billharz S (eds) Sustainable indicators: report of the project of indicators of sustainable development. John Wiley & Sons, New York, pp 13–27
- Gianisa A, Le De L (2018) The role of religious beliefs and practices in disaster: the case study of the 2009 earthquake in Padang city, Indonesia. *Disaster Prev Manag Int J* 27(1):74–86. <https://doi.org/10.1108/DPM-10-2017-0238>
- Gianisa A, Le De L (2018) The role of religious beliefs and practices in disaster: the case study of the 2009 earthquake in Padang city, Indonesia. *Disaster Prev Manag Int J* 27(1):74–86. <https://doi.org/10.1108/DPM-10-2017-0238>
- Ho M, Lall U, Allaire M, Devineni N, Kwon HH, Pal I, Raff D, Wegner D (2017) The future role of dams in the United States of America. *Water Resour Res* 53:982–998. <https://doi.org/10.1002/2016WR019905>
- Holand I, Lujala P, Ketil J (2011) Social vulnerability assessment for Norway: a quantitative approach. *Norsk Geografisk Tidsskrift—nor J Geogr* 65:1–17. <https://doi.org/10.1080/00291951.2010.550167>
- INE (2011) Censo de población y vivienda 2011. <http://www.ine.es/censos2011/tablas/Inicio.do>. Accessed 9 Jan 2017
- Kameshwar S, Cox DT, Barbosa AR, Farokhnia K, Park H, Alam MS, Van de Lindt JW (2019) Probabilistic decision-support framework for community resilience: Incorporating multi-hazards, infrastructure interdependencies, and resilience goals in a Bayesian network. *Reliab Eng Syst Saf* 191:106568. <https://doi.org/10.1016/j.ress.2019.106568>
- Kappes MS, Pappathoma-Köhle M, Keiler M (2012) Assessing physical vulnerability for multihazards using an indicator-based methodology. *Appl Geogr* 32(2):577–590. <https://doi.org/10.1016/j.apgeog.2011.07.002>
- Kelman I, Spence R (2004) An overview of flood actions on buildings. *Eng Geol* 73:297–309. <https://doi.org/10.1016/j.enggeo.2004.01.010>

- Koks EE, Jongman B, Husby TG, Botzen WJW (2014) Combining hazard, exposure and social vulnerability to provide lessons for flood risk management. *Environ Sci Policy* 47:42–52. <https://doi.org/10.1016/j.envsci.2014.10.013>
- Krellenberg K, Welz J (2017) Assessing urban vulnerability in the context of flood and heat hazard: pathways and challenges for indicator-based analysis. *Soc Indic Res* 132:709–731. <https://doi.org/10.1007/s11205-016-1324-3>
- Kryvasheyeu Y, Chen H, Obradovich N, Moro E, Van Hentenryck P, Fowler J, Cebrian M (2016) Rapid assessment of disaster damage using social media activity. *Sci Adv* 2(3):e1500779. <https://doi.org/10.1126/sciadv.1500779>
- Kumpulainen S (2006) Vulnerability concepts in hazard and risk assessment. In: Schmidt-Thome P (ed) *Natural and technological hazards and risks affecting the spatial development of European regions*. Geological Survey of Finland, Special paper. vol 42, p 65–74
- Leal M, Reis E, Pereira S, Santos PP (2021) Physical vulnerability assessment to flash floods using an indicator-based methodology based on building properties and flow parameters. *J Flood Risk Manag*. <https://doi.org/10.1111/jfr3.12712>
- Lin KHE, Lee HC, Lin TH (2017) How does resilience matter? An empirical verification of the relationships between resilience and vulnerability. *Nat Hazards* 88(2):1229–1250. <https://doi.org/10.1007/s11069-017-2916-1>
- Lundgren L, Jonsson A (2012) Assessment of social vulnerability. A literature review of vulnerability related to climate change and natural hazards. Centre for Climate Science and Policy Research, p 20
- Malakar S, Rai AK (2022) Earthquake vulnerability in the Himalaya by integrated multi-criteria decision models. *Nat Hazards* 111:213–237. <https://doi.org/10.1007/s11069-021-05050-8>
- Malgwi MB, Fuchs S, Keiler M (2020) A generic physical vulnerability model for floods: review and concept for data-scarce regions. *Nat Hazard* 20(7):2067–2090. <https://doi.org/10.5194/nhess-20-2067-2020>
- Martín-González F, Heredia N (2011a) Complex tectonic and tectonostratigraphic evolution of an Alpine foreland basin: the western Duero basin and the related tertiary depression of the NW Iberian Peninsula. *Tectonophysics* 502:75–89. <https://doi.org/10.1016/j.tecto.2010.03.002>
- Martín-González F, Heredia N (2011b) Geometry, structures and evolution of the western termination of the Alpine-Pyrenean Orogen reliefs (NW Iberian Peninsula). *J Iber Geol* 37(2):103–120. https://doi.org/10.5209/rev_JIGE.2011.v37.n2.1
- Mazzorana B, Simoni S, Scherer C, Gems B, Fuchs S, Keiler M (2014) A physical approach on flood risk vulnerability of buildings. *Hydrol Earth Syst Sci* 18:3817–3836. <https://doi.org/10.5194/hess-18-3817-2014>
- Ministerio de Medio Ambiente (2001) Guía técnica para la elaboración de los planes de emergencia de presas. Ministerio de Medio Ambiente. p 164
- Mínguez A (2015) Análisis y evolución del relieve de los Montes de León y del Sector Occidental de la Cordillera Cantábrica mediante la aplicación de Modelos Digitales de Elevación (Unpublished PhD Thesis). Universidad de León (Spain)
- Ministerio de Fomento (2017) Cartociudad. <http://www.cartociudad.es/portal/>. Accessed 9 Jan 2017
- Miranda FN, Ferreira TM (2019) A simplified approach for flood vulnerability assessment of historic sites. *Nat Hazards* 96:713–730. <https://doi.org/10.1007/s11069-018-03565-1>
- Müller A, Reiter J, Weiland U (2011) Assessment of urban vulnerability towards floods using an indicator-based approach—a case study for Santiago de Chile. *Nat Hazard* 11:2107–2123. <https://doi.org/10.5194/nhess-11-2107-2011>
- Noradika Y, Lee S (2017) Assessment of social vulnerability to natural hazards in south Korea: case study for typhoon hazard. *Spat Inf Res* 25:99–116. <https://doi.org/10.1007/s41324-017-0082-x>
- ODC (2015) International Open Data Charter. <https://opendatacharter.net/principles>. Accessed 20 July 2021
- Papathoma-Köhle M, Cristofari G, Wenk M, Fuchs S (2019) The importance of indicator weights for vulnerability indices and implications for decision making in disaster management. *Int J Disaster Risk Reduct* 36:101103. <https://doi.org/10.1016/j.ijdrr.2019.101103>
- Papathoma-Köhle M, Schlögl M, Dosser L, Roesch F, Borga M, Erlicher M, Keiler M, Fuchs S (2022) Physical vulnerability to dynamic flooding: vulnerability curves and vulnerability indices. *J Hydrol* 607:127501. <https://doi.org/10.1016/j.jhydrol.2022.127501>
- Paquier A, Goutal N (2016) Dam and levee failures: an overview of flood wave propagation modeling. *La Houille Blanche-Revue Internationale De L'eau* 1:5–12. <https://doi.org/10.1051/lhb/2016001>
- PNOA (2020) CC BY 4.0 www.scene.es
- Ruiz M (2011) Vulnerabilidad territorial y evaluación de daños post-catástrofe: una aproximación desde la geografía del riesgo (Unpublished PhD Thesis). Universidad Complutense de Madrid (Spain)

- Sadeghi-Pouya A, Nouri J, Mansouri N, Kia-Lashaki A (2017) An indexing approach to assess flood vulnerability in the western coastal cities of Mazandaran, Iran. *Int J Disaster Risk Reduct* 22:304–316. <https://doi.org/10.1016/j.ijdrr.2017.02.013>
- Sanderson D, Cox D, Amini M, Barbosa A (2022) Coupled urban change and natural hazard consequence model for community resilience planning. *Earth's Future*. <https://doi.org/10.1029/2022EF003059>
- Scheuer S, Haase D, Meyer V (2011) Exploring multicriteria flood vulnerability by integrating economic, social and ecological dimensions of flood risk and coping capacity: from a starting point view towards an endpoint view of vulnerability. *Nat Hazards* 58(2):731–751. <https://doi.org/10.1007/s11069-010-9666-7>
- Sim T, Hung LS, Su GW, Cui K (2018) Interpersonal communication sources and natural hazard risk perception: a case study of rural Chinese village. *Nat Hazards* 94:1307–1326. <https://doi.org/10.1007/s11069-018-3478-6>
- Singh A, Kanungo D, Pal S (2019) Physical vulnerability assessment of buildings exposed to landslides in India. *Nat Hazards* 96:753–790. <https://doi.org/10.1007/s11069-018-03568-y>
- Susha I, Grönlund A, Van Tulder R (2019) Data driven social partnerships: exploring an emergent trend in search of research challenges and questions. *Gov Inf Q* 36:112–128. <https://doi.org/10.1016/j.giq.2018.11.002>
- Tascón-González L, Ferrer-Julà M, Ruiz M, García-Meléndez E (2020) Social vulnerability assessment for flood risk analysis. *Water* 12(2):558. <https://doi.org/10.3390/w12020558>
- Tascón-González L (2017) Análisis metodológico para la estimación de la vulnerabilidad por inundaciones. Ejemplo de aplicación en el municipio de Ponferrada (León, España) (Unpublished PhD Thesis). Universidad de León (Spain)
- Terti G, Ruin I, Anquetin S, Gourley JJ (2015) Dynamic vulnerability factors for impact-based flash flood prediction. *Nat Hazards* 79:1481–1497. <https://doi.org/10.1007/s11069-015-1910-8>
- Thouret JC, Ettinger S, Guitton M, Santoni O, Magill C, Martelli K, Zuccaro G, Revilla V, Charca JA, Arguedas A (2014) Assessing physical vulnerability in large cities exposed to flash floods and debris flows: the case of Arequipa (Peru). *NatUtal Hazards* 73:1771–1815. <https://doi.org/10.1007/s11069-014-1172-x,2014>
- UNDRO (1980) Natural disasters and vulnerability analysis. Office of the United Nations Disaster Relief Coordinator, Geneva, p 64
- UNISDR- United Nations International Strategy for Disaster Reduction (2005) Hyogo Framework for Action 2005–2015: Building the Resilience of Nations and Communities to Disasters. Extract from the Final Report of the World Conference on Disaster Reduction (A/CONF. 206/6), Vol. 380, The United Nations International Strategy for Disaster Reduction, Geneva. Available at <https://www.unisdr.org/2005/wcdr/intergover/official-doc/L-docs/Hyogoframework-for-action-english.pdf>
- Usman Kaoje I, Abdul Rahman MZ, Idris NH, Tam TH, Mohd Sallah MR (2021) Physical flood vulnerability assessment of buildings in Kota Bharu, Malaysia: an indicator-based approach. *Int J Disaster Resil Built Environ* 12(4):413–424. <https://doi.org/10.1108/IJDRBE-05-2020-0046>
- Vargas J (2002) Políticas públicas para la reducción de la vulnerabilidad frente a los desastres naturales y socio-naturales. Naciones Unidas, CEPAL, p 84
- Velev D, Zlateva P (2012) Use of social media in natural disaster management. *Intl Proc Econ Dev Res* 39:41–45
- Wang Z, Ye X (2018) Social media analytics for natural disaster management. *Int J Geogr Inf Sci* 32(1):49–72. <https://doi.org/10.1080/13658816.2017.1367003>
- Weichselgartner J (2001) Disaster mitigation: the concept of vulnerability revisited. *Disaster Prev Manag* 10(2):85–94. <https://doi.org/10.1108/09653560110388609>
- Weichselgartner J (2002) About the capacity to be wounded: the need to link disaster mitigation and sustainable development. In: Tetzlaff G, Trautmann T, Radtke KL (eds) *Extreme Naturereignisse-Folgen, Vorsorge, Werkzeuge*. German Committee for Disaster Reduction (DKKV), Bonn, pp 150–158
- World Imagery (2017) World Imagery ESRI. <https://www.arcgis.com/home/item.html?id=10df2279f9684e4a9f6a7f08febac2a9>. Accessed 16 May 2017
- World Street Map (2017) World Street Map. ESRI. <https://www.arcgis.com/home/item.html?id=3b93337983e9436f8db950e38a8629af>. Accessed 16 May 2017
- Xing Z, Yang S, Zan X, Dong X, Yao Y, Liu Z, Zhang X (2023) Flood vulnerability assessment of urban buildings based on integrating high-resolution remote sensing and street view images. *Sustain Cities Soc* 92:104467. <https://doi.org/10.1016/j.scs.2023.104467>
- Zuiderwijk A, Janssen MFWHA (2014) The negative effects of open government data - investigating the dark side of open data. In: *Proceedings of the 15th annual international conference on digital government research*. Association for Computing Machinery (ACM), p 147–152

Publisher's Note Springer Nature remains neutral with regard to jurisdictional claims in published maps and institutional affiliations.